

# Delay and dispersion in the microvascular network due to laminar flow with account for vessel bifurcations

Elias Kellner<sup>1</sup>, Roman Fleyshe<sup>2</sup>, Matthias Günther<sup>3</sup>, Marco Reiser<sup>1</sup>, Peter Gall<sup>1</sup>, and Valerij G. Kiselev<sup>1</sup>

<sup>1</sup>Department of Radiology, University Hospital Freiburg, Freiburg, Germany, <sup>2</sup>Gruss Magnetic Research Center, Department of Radiology, Albert Einstein College of Medicine, Bronx, NY, United States, <sup>3</sup>Institute for Medical Image Computing, Fraunhofer MEVIS, 28359, Germany

**Target Audience:** Perfusion Community (DCE, DSC, ASL, PET, CT)

**Introduction:** Tracer kinetic models relate tracer concentrations at different points in the blood stream. Accounting for blood transport between such points is crucial for correct modeling and quantitative analysis of pharmacokinetic and perfusion data in DSC, DCE ASL MRI and CT/PET. Delay and dispersion in bolus-tracking perfusion measurements is a notorious example lacking a theoretical model. It is widely accepted now that delay and dispersion arise in virtually any vessel due to different blood velocities in the laminar flow<sup>1-3</sup>. Here we propose a way to account for vessel bifurcations thus expanding theoretical description from individual vessel segments to large microvascular trees. Engaging the scaling model of vascular architecture results in coupling of delay and dispersion and yields a simple form for the kernel of kinetic models.

**Theory:** We treat the vascular network as a tree consisting of straight cylindrical segments between successive bifurcations. Transport through each segment is described by a distribution  $h(\tau)$  of transit times  $\tau$ . Major assumption of the present model is good mixing of blood at bifurcations, at least in a statistical sense in large vascular networks. Good mixing at bifurcations leads to statistical independence of particles' velocities in different segments. Consequently, the distribution of transit times for a chain of  $N$  segments,  $h_{1-N}(\tau)$ , is given by a convolution chain of distributions for individual segments,  $h_{1-N}(\tau) = h_N(\tau) \otimes \dots \otimes h_2(\tau) \otimes h_1(\tau)$ .

The second major point of the present method is the dependence of the apparent tracer concentration on the measurement scheme. There are two basic types of measurements. One is a snapshot acquisition in which the resulting tracer concentration is the spatial mean of all laminae in a selected cross-section of a vessel with equal weights. This is typical for fast MRI. The other basic type is flow measurement in which blood is mixed at the measurement site, for example, by collecting it in a vessel. The tracer concentration is thus a mean in which contributions of individual laminae are weighted with their velocities. This kind of mean concentration forms the above convolution chain.

Further analysis is performed for the laminar flow with parabolic velocity profile. The central quantity is a stem function,  $H(t, x)$  which is the tracer concentration in a long cylinder after an instant labeling of blood for all  $x < 0$  (cf. PASL). For the snapshot measurement  $H(t) = 1 - t_0/t$  for  $t > t_0$ , where  $t_0$  is the bolus arrival time. For the flow-type measurement,  $H(t) = 1 - t_0^2/t^2$  for  $t > t_0$ . Realistic labeling boli are obtained by an appropriate linear combination of these functions. In general, the impulse response to the incoming tracer concentration is the time derivative of  $H(t)$ . This gives  $h(\tau) = 2t_0^3/\tau^3$  for  $\tau > t_0$  for the flow-type measurements and  $h(\tau) = t_0^2/\tau^2$  for the snapshot type.

In the simplest plausible model of vascular architecture as a self-similar dichotomic tree obeying Murray's law<sup>4</sup>,  $h(\tau)$  does not depend on the vessel generation and the convolution chain turns to a power of this function in the Fourier domain.

The limits of the present model are set by flow pulsations in large arteries and poor applicability of statistics on this level. Applicability of the explicit model for  $h(\tau)$  for a parabolic flow profile is limited by the mixing by erythrocytes and molecular diffusion in small vessels of the order of tens of micrometers. The model is thus applicable to the major middle part of the vascular tree.

**Experiments** began with investigation of usefulness of large arteries for verification of the developed theory. The brain of a volunteer was imaged using single-shot 3D-GRASE sequence<sup>5</sup> at a 3T scanner. A time series was acquired with 60 time steps starting at TI = 100 ms with an increment of 50 ms. The saturation RF pulses was applied 500 ms after labeling. Morphological information was obtained using a 3D-TOF-MRA.

**Experimental results:** We segmented two paths (Fig.1), calculated the ASL bolus along each path and fitted the model to ASL data by adjusting only the incoming central-streamline velocity with results  $v_0 = 41$  and  $43$  cm/s for the left and right path (Fig.1), respectively. Inserts in Fig.1 show the first moment of ASL signal vs. the length along each path. Black lines show the model prediction. The saw-tooth structure results from mixing at bifurcations. Fig.2 shows the best (right column) and the worst (left column) fitting in voxels from each segment (colors from Fig.1) of the longer left path. Analysis of signals from the right vessel path in Fig.1 yields similar results.

**Discussion:** The proposed model of blood transport combined with a statistical model of microvasculature yields an analytical description of kernel  $h(t)$ , the central quantity of tracer kinetics models. Our theoretical framework can accommodate other, more precise models of microvasculature as well. The present model with its single, physically meaningful parameter allows for prediction of the transport function to high vessel generations, which are not easily accessible to direct measurements. Application of the developed model to ASL with this single fitting parameter for all curves along a path leads to reasonable results. However, this is not decisive for model selection (Fig.3 illustrates a good fitting quality of three radically different models in the same voxel). Even the parameter outcome of fitting can be insufficient, e.g., a replacement of the present model  $h(\tau) = 2t_0^3/\tau^3$  with  $h(\tau) = t_0^2/\tau^2$  results in  $v_0 = 51$  and  $56$  cm/s and even in a slight increase in the fitting quality. The latter can be explained by the effect of pulsations which broaden the plots in Fig.2 and make the  $1/\tau^2$  model with its broader bolus more favorable. Note that the models with  $h \sim 1/\tau^2$  result in a divergent, i.e. non-existing mean transit time, a problem absent in our model.

**References:** [1] Gall et al, proc. ISMRM 2008 #627, 2010 #1795, 1736. [2] Gallichan, Jezzard, MRM 2008;60(1):53-63. [3] Okell et al., MRM 68:969-979 (2012). [4] Turner, NeuroImage 2002;16(4):1062-7. [5] Gunther et al., MRM 2005;54(2):491-498.

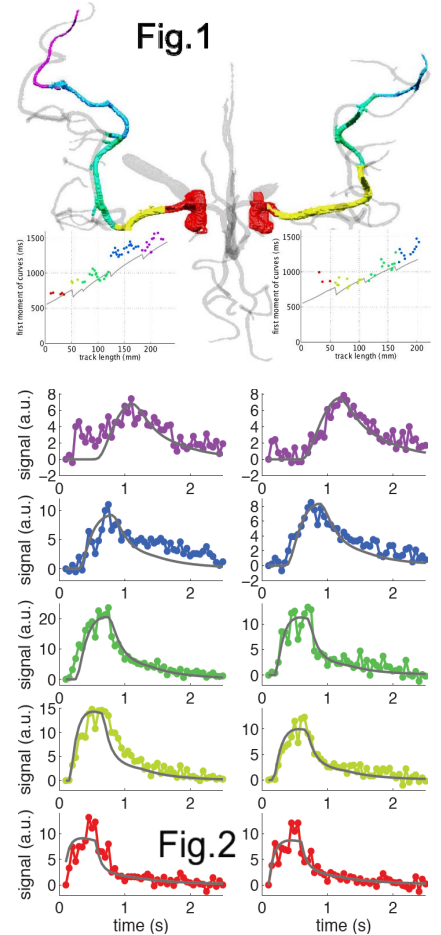


Fig.1

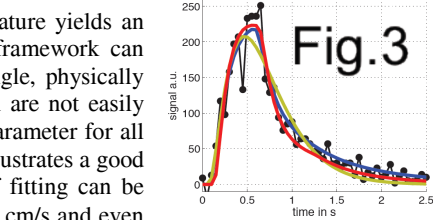


Fig.2

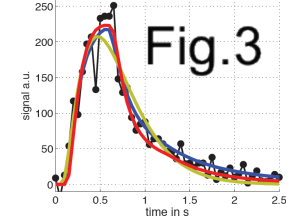


Fig.3

Fitting result in one voxel for three different models: red:  $h(\tau) = 2t_0^3/\tau^3$  blue:  $h(\tau) = t_0^2/\tau^2$  brown: gamma